11,05

Magnetic and Mössbauer Studies of Nanocomposites with Carbidosteels Composition doped by Chromium and Nickel

© A.A. Chulkina, A.I. Ulyanov, A.L. Ulyanov, V.E. Porsev

Udmurt Federal Research Center, Ural Branch Russian Academy of Sciences, Izhevsk, Russia

E-mail: chulkina@udman.ru

Received July 27, 2023
Revised July 27, 2023
Accepted August 5, 2023

The properties of alloys $(Fe_{0.95-y}Cr_{0.05}Ni_y)_{83}C_{17}$ and $(Fe_{0.90-y}Cr_{0.10}Ni_y)_{83}C_{17}$, where $y = 0.05$ and 0.10, obtained by mechanosynthesis and subsequent annealing, were studied by Mössbauer spectroscopy and magnetic measurements, using X-ray diffraction data. As a result of annealing at 500°C, nanocomposites are formed with a similar phase composition (cementite and austenite matrix with the ferrite inclusions) and maximum values of the coercive force H_c. At the same time, H_c of high-chromium composites is more than two times higher than H_c of low-chromium composites (210−250 and 100 A/cm, respectively). Mössbauer studies have shown that the cementite of high-chromium alloys is in a paramagnetic state, while that of low-chromium alloys is in a ferromagnetic state. This aspect determines the features of magnetization reversal of close to the critical single-domain size ferrite inclusions, which leads to different maximum values of H_c for low- and high-chromium nanocomposites.

Keywords: transition metals, mechanosynthesis, nanostructured materials, phase transitions, saturation magnetization, coercive force, Mössbauer spectroscopy.

DOI: 10.61011/PSS.2023.10.57230.160

1. Introduction

In industry, carbidosteels are widely used, they consist of a binder phase and hard carbides with a mass fraction of 20 to 70%, which in terms of strength characteristics occupy an intermediate position between steels and hard alloys. Carbidosteels are most often produced by powder metallurgy, and the grain size of the solid phase is usually in the micrometer region [1]. According to modern concepts, the maximum strength characteristics are found in alloys which grain sizes are in the nanometer range [2]. These requirements are met by alloys prepared by mechanical synthesis (MS) in planetary ball mills [3]. Mechanically synthesized alloys are a convenient model material for studying the patterns of changes in the nanostructural state of alloys during heat treatments, doping, irradiation and other types of physical effects. It is known [4] that in the process of mechanosynthesis of iron-carbon alloys, the amorphous phase is usually formed, as well as crystalline nanoscale phases, which are in a non-equilibrium stress-strain state with strong distortions of their crystal lattices. During annealing crystallization of the amorphous phase with the formation of cementite and other carbides, the removal of distortions of the crystal lattices of the phases, and an increase in the size of their nanograins occur. To improve operational and technological characteristics the alloys are doped. The phase composition and structural state of phases after MS and annealing are most often determined by X-ray diffraction. Additional information on the magnetic state of the phases of mechanosynthesized alloys and their doping can be provided by Mössbauer studies, as well as by measuring such magnetic characteristics as specific saturation magnetization σ_s, coercive force H_c, magnetic susceptibility χ.

For the first time the magnetic properties of one of the main phases of mechanosynthesized carbidosteels — cementite Fe_3C — were studied in the paper [5]. It turned out that the coercive force of cementite varies from 80 (in the state after MS) to 240 A/cm (after annealing at 500°C). Annealing at higher temperatures again reduces H_c of cementite. The low value H_c of cementite after MS is due, firstly, to the fact that in the highly distorted crystal lattice of cementite the carbon atoms can be located not only in prismatic, but also in non-equilibrium octahedral positions of its lattice. This causes a significant decrease in the magnetocrystalline anisotropy constant K of cementite [6] and, consequently, determines its low value H_c. This may also be facilitated by the low values of the coercive force of the amorphous phase and ferrite, which are usually present in the alloys under discussion at the end of MS. Annealing at 500°C removes lattice distortions, which ensures the transition of carbon atoms to equilibrium prismatic positions, thus restoring the constant K of cementite. The high value of the constant K and a sufficiently high density of linear defects in the crystal structure lead to the maximum value of H_c of cementite after annealing at 500°C. Annealing at temperature of $T_{ann} > 500$°C due to intense decrease in the density of defects in the crystal structure again reduce H_c of cementite.

Doping affects not only the strength, but also the magnetic characteristics of individual phases and alloys as a whole. For example, doping by chromium reduces coercive force H_c, specific saturation magnetization σ_s and Curie

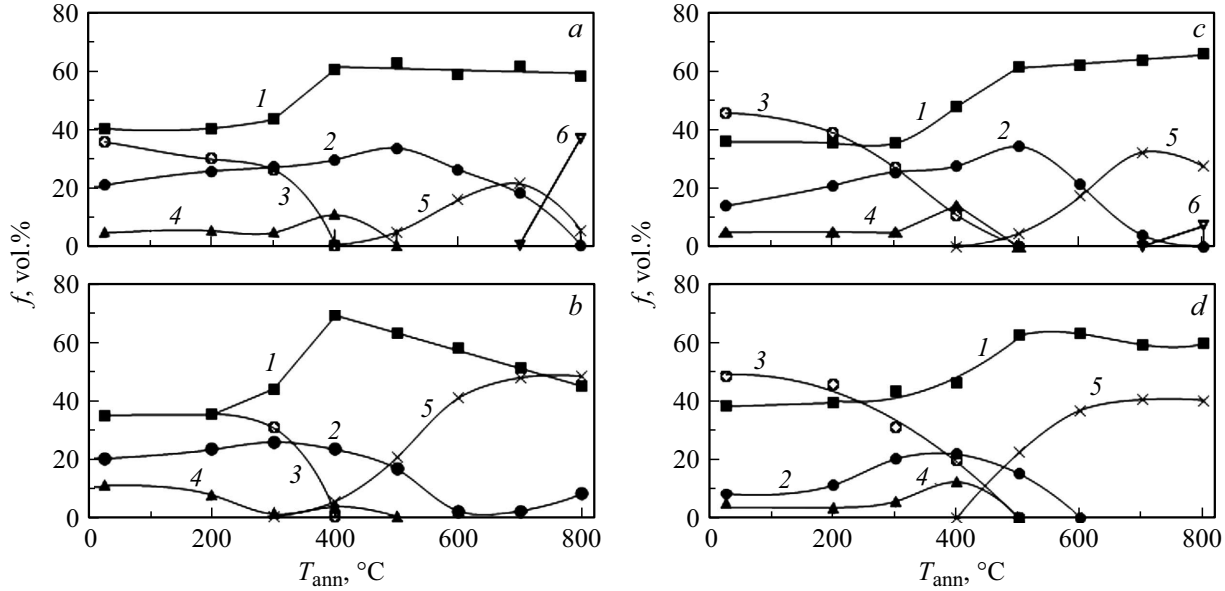

Figure 1. Phase composition f of alloys vs. annealing temperature T_{ann}: *a* — $(Fe_{0.90}Cr_{0.05}Ni_{0.05})_{83}C_{17}$; *b* — $(Fe_{0.85}Cr_{0.05}Ni_{0.10})_{83}C_{17}$; *c* — $(Fe_{0.85}Cr_{0.10}Ni_{0.05})_{83}C_{17}$; *d* — $(Fe_{0.80}Cr_{0.10}Ni_{0.10})_{83}C_{17}$. Phases: *1* — cementite, *2* — ferrite (α-Fe), *3* — amorphous phase, *4* — χ-carbide, *5* — austenite, *6* — martensite.

temperature T_C of cementite [7,8]. Doping by nickel also reduces H_c and σ_s, but increases T_C of cementite [9,10].

In [11] the MS method was used to obtain carbidosteels doped by chromium and nickel with the $(Fe, Cr, Ni)_{83}C_{17}$ composition. It was shown that after annealing carbidosteels were composites consisting of a solid phase — nano-sized cementite and binder phase — austenite. This paper presents the results of the magnetic properties study of composites obtained in [11]. In particular, the influence of the structural state of ferrite and the magnetic state of cementite on the formation of magnetic characteristics of the alloys under study is discussed.

2. Samples and methods of investigation

Samples of nanocomposites with carbidosteel composition were prepared using the MS method. For this end the mixture of powders of carbonyl iron (purity 99.98%), nickel and chromium (purity 99.9%), graphite (purity 99.99%), taken in the ratio of $(Fe_{0.95-y}Cr_{0.05}Ni_y)_{83}C_{17}$ and $(Fe_{0.90-y}Cr_{0.10}Ni_y)_{83}C_{17}$, where $y = 0.05$ and 0.10, was subjected to high energy milling for 16 h in argon atmosphere in „Pulverisette-7“ planetary ball mill. The energy intensity of the mill was 2.0 W/g. The platform rotation speed is 74 rad/s. The grinding balls and vessels were made of steel ShKh15. The ratio of the mass of grinding balls with diameter of 8 mm to the mass of the loaded powder is 7 : 1. The weight increasing of the powder due to the milling yield of iron from the surface of the balls and walls of vessels is — maximum 1−3%. The average size of particles of the composite powder after mechanosynthesis was $\approx 5\,\mu$m.

Powder samples were annealed in argon atmosphere for 1 h on the setup for measuring the temperature dependence of magnetic susceptibility. The amplitude of the probing alternating field was 1.25 A/cm, frequency — 120 Hz. The rate of heating and cooling of samples is — 30°C/min.

To study the state and properties of the obtained composites X-ray diffraction analysis, Mössbauer spectroscopy and magnetic measurements were used. X-ray diffraction analysis was carried out at room temperature on a Rigaku Miniflex 600 diffractometer in the Bragg-Brentano geometry using Co-Kα radiation. Mössbauer spectra were obtained at room temperature in the mode of constant accelerations of the γ-radiation source ^{57}Co(Rh) on SM2201DR spectrometer. Discrete processing of the spectra was carried out using the least-squares method according to Levenberg–Marquardt algorithm. Mathematical processing of the spectra in continuous representation in order to restore the distribution function of hyperfine magnetic fields was performed in a single-core model using a generalized regularized algorithm for solving inverse incorrect problems [12]. The magnetic characteristics of the samples were measured on a vibrating magnetometer with a maximum magnetizing field of 13 kA/cm.

3. Results and their discussion

Phase composition of low chromium $(Fe_{0.95-y}Cr_{0.05}Ni_y)_{83}C_{17}$ and igh chromium $(Fe_{0.90-y}Cr_{0.10}Ni_y)_{83}C_{17}$ alloys where $y = 0.05$ and 0.10, after mechanosynthesis and further annealing, is shown in Figure 1. After MS alloys consist of amorphous phases (35−50 vol.%) and nanoscale non-equilibrium phases: cementite mainly doped by Cr and ferrite mainly doped by

N, and also small amount of χ-carbide $(Fe, Cr, Ni)_5C_2$ [11]. During annealing up to 400–500°C due to the large value of internal energy of MS-alloys the intensive phase transformations are occur: amorphous phase (curves *3*) crystallizes with formation of cementite (curves *1*), χ-carbide (curves *4*) and ferrite (curves *2*), χ-carbide converts into cementite. Annealing at higher temperatures leads to the austenite formation (curves *5*). As a result of annealing at temperature $T_{ann} \geq 500$°C, composites are formed, consisting mainly of cementite, ferrite and austenite. In low-nickel alloys $(Fe_{0.90}Cr_{0.05}Ni_{0.05})_{83}C_{17}$ and $(Fe_{0.85}Cr_{0.10}Ni_{0.05})_{83}C_{17}$ during cooling after annealing at 800°C martensite (curves *6*, Figure 1 *a*, 1 *c*) is formed in amount of up to 20 and 8 vol.%, respectively. In high-nickel alloys after annealing at 700–800°C ferrite may reappear again due to the decomposition of cementite.

Phase and structural changes that occur during MS and subsequent annealing determine the magnetic properties of nanocomposites. Figure 2, *a* shows that after MS the values of the specific saturation magnetization σ_s of high-chromium alloys (curves *3, 4*) are significantly lower than that of low-chromium alloys (curves *1, 2*). This is due to the fact that in high-chromium alloys, compared to low-chromium alloys, the content of highly magnetic ferrite is significantly lower (Figure 1). Another reason for the lower values of σ_s of high-chromium alloys is the more intensive doping of their cementite by chromium [7,13].

After annealing up to 400°C, the specific magnetization of the alloys, despite the occurring phase changes (Figure 1), remains practically unchanged (Figure 2, *a*). Apparently, in this annealing temperature range the decrease in the magnetic moment of some phases, for example, the disappearance of the amorphous phase, is compensated by increase in the magnetic moments of other phases. Significant decrease in σ_s of alloys is observed after annealing at $T_{ann} > 500$°C, when intensive redistribution of doping elements (Cr and Ni) starts, which are located in large quantities in segregations along grain boundaries. In particular, the decrease in σ_s of composites in the range T_{ann} from 400–500 to 700°C is mainly due to active doping of cementite by Cr atoms, as well as the appearance and subsequent increase in the volume of paramagnetic austenite (Figure 1, curves *5*). After annealing at 700–800° C all composites, excluding $(Fe_{0.90}Cr_{0.05}Ni_{0.05})_{83}C_{17}$ become weakly magnetic (Figure 2, *a*). High value of σ_s of the composite $(Fe_{0.90}Cr_{0.05}Ni_{0.05})_{83}C_{17}$ is due to formation of highly magnetic martensite during cooling of this alloy after annealing at 800°C.

Phase and structural changes that occur during MS and annealing determine the coercive force $H_c$of the nanocomposites under study (Figure 2, *b*). After mechanosynthesis H_c of alloys is 20–25 A/cm, which is much lower than H_c of mechanosynthesized cementite Fe_3C [5]. This is explained, firstly, by the doping of phases of the composites by chromium and nickel, which reduce their H_c [7,9]. Secondly, they contain rather high content (from 8 to 40 vol.%) of soft magnetic amorphous and ferrite

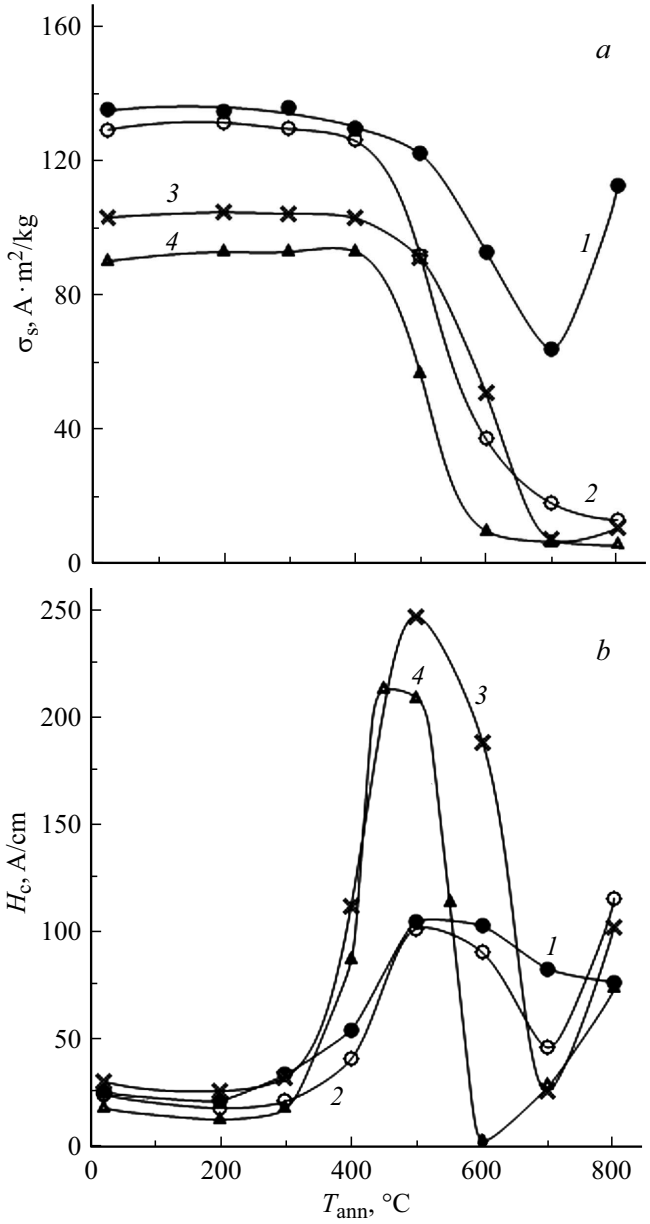

Figure 2. dependence on annealing temperature T_{ann}: *a* — specific saturation magnetization σ_s and *b* — coercive force H_c of alloys: *1* — $(Fe_{0.90}Cr_{0.05}Ni_{0.05})_{83}C_{17}$; *2* — $(Fe_{0.85}Cr_{0.05}Ni_{0.10})_{83}C_{17}$; *3* — $(Fe_{0.85}Cr_{0.10}Ni_{0.05})_{83}C_{17}$; *4* — $(Fe_{0.80}Cr_{0.10}Ni_{0.10})_{83}C_{17}$.

phases (Figure 1). The dependences of the coercive force on the annealing temperature $H_c(T_{ann})$ of the studied alloys are curves with maximum in the region of $T_{ann} \approx 500$°C (Figure 2, *b*). High maximum values H_c of high-chromium composites (curves *3, 4*) in relation to low-chromium composites (curves *1, 2*) turn heads, although their phase composition after annealing at 500°C is approximately the same (compare the content of phases in the alloys shown in Figure 1, *a, c* and 1, *b, d*). To clarify this situation, information is needed on the magnetic state of the phases of the composites under study, which was obtained from Mössbauer measurements.

Table 1. (Mössbauer parameters of spectrum components of composites $(Fe_{100-X-Y}Cr_XNi_Y)_{83}C_{17}$ at various annealing temperatures obtained as result of processing in discrete representation: (*IS* — isomeric shift, *QS* — quadrupole splitting, $\Gamma_{1,6}$ — width *1* and *6* of line, *S* — portion of iron atoms in phase, $\langle H\rangle$ — average hyperfine magnetic field on nuclei ^{57}Fe)

Composition of composite (X; Y)	Paramagnetic phases					Ferromagnetic phases				
	Austenite		Cementite			Ferrite		Austenite/cementite*		
			Doublet1/Doublet2							
	IS, mm/s	S,%	IS, mm/s	QS, mm/s	S, %	$\langle H\rangle$, kOe	S, %	$\langle H\rangle$, kOe	$\Gamma_{1,6}$, mm/s	S, %
Table 1, *a*. $T_{ann} = 500°C$										
0.10; 0.10	−0.14	4	0.12/0.16	0.61/0.36	59	337	30	118	0.44	7
0.10; 0.05	–	–	0.13/0.15	0.82/0.42	51	338	47	112	0.44	2
Table 1, *b*. $T_{ann} = 800°C$										
0.10; 0.10	−0.14	31	0.18/0.19	0.49/0.22	64	341	1	114*	0.32*	4*
0.05; 0.10	−0.13	37	0.20/0.17	0.49/0.30	42	339	18	88*	0.41*	3*

Let's discuss alloys with increased content of chromium. Figure 3, *a* shows the Mössbauer spectrum and function $P(H)$ of annealed at 500°C high-chromium nanocomposite $(Fe_{0.80}Cr_{0.10}Ni_{0.10})_{83}C_{17}$. Function $P(H)$ of spectrum reflects the distribution of hyperfine magnetic fields on the nuclei of iron isotopes from atoms in the nearest neighborhood. Analysis of this function showed that $\approx 37\%$ of all Fe atoms are in ferromagnetic and $\approx 63\%$ in paramagnetic phases.

Processing of Mössbauer spectra in a discrete representation allows one to obtain more detailed information about the magnetic state of individual phases of composites. The results of such processing of the alloy under discussion are given in Table 1, *a* (top line). Some uncertainty appears in recognizing the component *3* (Figure 3, *a*) with broad lines and average hyperfine magnetic field $\langle H\rangle \approx 118$ kOe, in which $\approx 7\%$ of atoms Fe present. From the comparison of the results of X-ray diffraction analysis to determine the volumetric content of austenite in the alloy (≈ 22 vol.%, Figure 1, *d*), Mössbauer spectroscopy data on the content of Fe atoms in the paramagnetic austenite ($\approx 4\%$) and taking into account [14] it follows that the component *3* should be attributed to Ni-doped ferromagnetic austenite.

Similar pattern relating magnetic condition of phases, excluding austenite, is observed also for sample $(Fe_{0.85}Cr_{0.10}Ni_{0.05})_{83}C_{17}$, annealed at 500° C (Table. 1, *a*, lower line). From Figure 3, *b* (left) we can conclude that spectrum of this composite does not contain paramagnetic component of austenite. Consequently, all austenite formed in the alloy (Figure 1, *c*, curve *5*) should be ferromagnetic. To prove this, we subtracted the component from ferrite from the spectrum of the alloy. In the resulting spectrum (see Figure 4), broadened lines of the sextet are clearly visible near the base of the paramagnetic doublet. This indicates the presence in the spectrum of the magnetically split component with an average hyperfine magnetic field $\langle H\rangle = 112$ kOe, which we identify as ferromagnetic austenite.

The presence in the Mössbauer spectra of high-chromium alloys, annealed at 500°C, magnetically split austenite components with an average hyperfine magnetic field $\langle H\rangle \approx 110-120$ kOe, indicates a low saturation magnetization of this phase. The coercive force of such austenite is close to H_c of ferrite. Thus, the discussed composites mainly contain ferrite and paramagnetic phases (cementite + austenite). There is also a small amount of ferromagnetic austenite with low saturation magnetization.

Ferrite under normal conditions is a soft magnetic phase with H_c maximum 5−10 A/cm [15]. Therefore, the experimentally observed high maximum values $H_c \approx 210-240$ A/cm (Figure 2, *b*, curves *3, 4*) of high-chromium composites can be explained if we assume that, firstly, the sizes of ferromagnetic inclusions of ferrite after annealing at 500°C are close to the critical size of their single domain d_{cr}. So, according to [16] critical size d_{cr} of single domain of particlesα-Fe is (21 ± 3) nm, at this their $H_c > 500$ A/cm. The deviation of the average sizes of iron particles from the value d_{cr} in one direction or another significantly reduces their H_c. If iron particles are doped by nickel, their d_{cr} may have higher values, since for nickel $d_{cr} \approx (72 \pm 5)$ nm [16]. Secondly, ferrite inclusions shall be distant from each other or magnetically isolated, for example, by layers of paramagnetic phases. Let us discuss the fulfillment of these assumptions for high-chromium composites.

For nanocrystalline materials the average size of coherent scattering regions $\langle D\rangle$, determined by X-ray diffraction, is close to the size of its grains. Figure 5 (curve *1*) presents dependence $\langle D\rangle$ of ferrite of high chromium alloy $(Fe_{0.80}Cr_{0.10}Ni_{0.10})_{83}C_{17}$ on annealing temperature. It can be seen that after the alloy annealing at 500°C for Ni-doped ferrite $\langle D\rangle \approx 60$ nm, which is apparently close to the critical size of its single domain d_{cr}.

It is known [17] that the formation of the nanostructured state of materials is accompanied by the formation of significant proportion of high-angle grain boundaries. The

nanostructural state of the initial components (powders α-Fe, Cr, Ni, graphite) of the alloys under discussion is realized practically at the initial stage of mechanosynthesis. Next, carbon atoms penetrate, and then atoms of doping elements along the grain boundaries of nanostructured α-Fe and their adsorption on the grain boundaries with the formation of segregations. As a result, an amorphous Fe-Cr-Ni-C phase is formed at interfaces containing boundary and close-to-boundary distorted zones. During the mechanosynthesis some sections of the amorphous phase, which reach the composition $(Fe, Cr, Ni)_{75}C_{25}$, crystallize with the cementite formation. Crystallization of the amorphous phase remaining after mechanosynthesis completion occurs during annealing with the formation of cementite doped mainly by chromium and ferrite doped mainly by Ni. Nickel can be included in cementite, but in a very limited amount [9]. Nickel, which could not dissolve in ferrite, is located in the interface region of grains α-Fe (ferrite), including in the form of segregations, and participates in the austenite formation during annealing. As a result of annealing of high-chromium alloys at temperature of 500°C, austenite is formed on the surface of some ferrite grains, around which a sufficient number of nickel atoms are concentrated. In the alloy with reduced nickel content this austenite is ferromagnetic, with low specific saturation magnetization (weakly magnetic). The alloy with high nickel content contains both weakly magnetic and paramagnetic austenite. All ferrite grains, both with and without the presence of austenite on their surface, are surrounded by paramagnetic cementite. The main contribution to the formation of high values of the coercive force of high-chromium alloys annealed at 500°C is provided by the magnetization reversal of single-domain ferrite inclusions (without the presence of ferromagnetic austenite), which are surrounded by paramagnetic phases. This magnetization reversal occurs through irreversible coherent rotation of magnetization [15]. In this case, H_c of ferrite inclusions becomes maximum. There will most likely be an exchange interaction between ferrite inclusions and weakly magnetic austenite, which will contribute to the formation of the coercive force of the composite, reducing its value. However, this contribution will not be decisive. The increase in the ferromagnetic austenite content in high-nickel alloy, compared to low-nickel alloy (according to Mössbauer data, 7% and 2% Fe atoms are contained in such alloys, respectively), does not lead to a significant change in the value of H_c of the alloys annealed at $T_{ann} = 500$°C. Thus, the combined action of magnetization reversal mechanisms through irreversible coherent rotation of the magnetization of single-domain ferrite inclusions and incoherent Magnetization reversal of ferrite and ferromagnetic austenite inclusions in exchange interaction provides high value of the coercive force of high-chromium composites, equal to 210−240 A/cm (Figure 2, *b*, curves *3, 4*).

The coercive force of high-chromium composites after annealing in the temperature range of 500 to 600−700°C significantly decreases (Figure 2, *b*, curves *3, 4*). As follows from Figure 1, *c* and 1, *d*, the volume of austenite in this range T_{ann} increases (curves *5*), and the ferrite content (curve *2*) and the average size of its inclusions (curve *1* in Figure 5) decrease. This leads to a gradual transition of ferrite particles into superparamagnetic state, which causes a sharp decrease in H_c of ferrite and, consequently, in the coercive force of the samples. Thus, the coercive force of high-chromium composites in the range T_{ann} of 500−600 to 700°C is determined mainly by the average size of ferrite inclusions [15] surrounded by paramagnetic phases.

A different situation in the formation of maximum values H_c occurs for low-chromium composites. Figure 3, *c* and 3, *d* show Mössbauer spectra and functions $P(H)$ of composites $(Fe_{0.90}Cr_{0.05}Ni_{0.05})_{83}C_{17}$ and $(Fe_{0.85}Cr_{0.05}Ni_{0.10})_{83}C_{17}$, annealed at 500°C. The shape of the spectra indicates the presence of several ferromagnetic phases in the composites. The analysis of function $P(H)$ of alloy $(Fe_{0.90}Cr_{0.05}Ni_{0.05})_{83}C_{17}$ indicates that ≈ 41% of all Fe atoms of the composite contained in ferrite doped mainly by nickel, this is confirmed by peak of function $P(H)$ at the field of $H \approx 337$ kOe. About 56% of all Fe atoms are contained in ferromagnetic cementite doped mainly by chromium, the distribution of its function $P(H)$ is in the range of fields $H \approx (50-210)$ kOe. Rest Fe atoms (about 3%) are included in paramagnetic austenite (small value of its function $P(H)$ is observed in the field of $H = 0$ kOe (Figure 3, *c*)).

Composite phases with increased nickel content $(Fe_{0.85}Cr_{0.05}Ni_{0.10})_{83}C_{17}$ after similar heat treatment have, with the exception of austenite, a similar magnetic state (Figure 3, *d*). Austenite, the content of which in this composite is about 20 vol.% (Figure 1, *b*), is partly in a paramagnetic and partly in a ferromagnetic state. Analysis of function $P(H)$ of composite showed that number of Fe atoms in paramagnetic austenite is ≈ 7% (Figure 3, *d*, distribution of function $P(H)$ is in the field of $H = 0$ kOe). The remaining Fe atoms of austenite are located in its ferromagnetic part. In this case, the function $P(H)$ of ferromagnetic austenite in the field range of 50 to 210 kOe is overlapped by the function $P(H)$ of ferromagnetic cementite (Figure 3, *d*). Figures 3, *c* and 3, *d* (left) also show the components of ferrite and components with a wide distribution of hyperfine magnetic fields, obtained by restoration from the spectrum of function $P(H)$. Thus, low-chromium composites after annealing at 500°C consist mainly of a mixture of two ferromagnetic phases-ferrite and cementite, which are most likely under conditions of exchange interactions.

Let's consider in detail the composite $(Fe_{0.85}Cr_{0.05}Ni_{0.10})_{83}C_{17}$, which contains 16 vol.% of ferrite and 63 vol.% of ferromagnetic cementite (Figure 1, *b*). The average grain size of ferrite and cementite of this composite after annealing at 500°C according to X-ray data is ≈ 48 (Figure 5, curve *2*) and 45 nm respectively. In this case, the average size of ferrite grains is most likely close to its single-domain state. The width of cementite domain walls according to [6] is $\delta \approx 6$ nm (for Cr-doped cementite δ it may be slightly higher). This means that the cementite

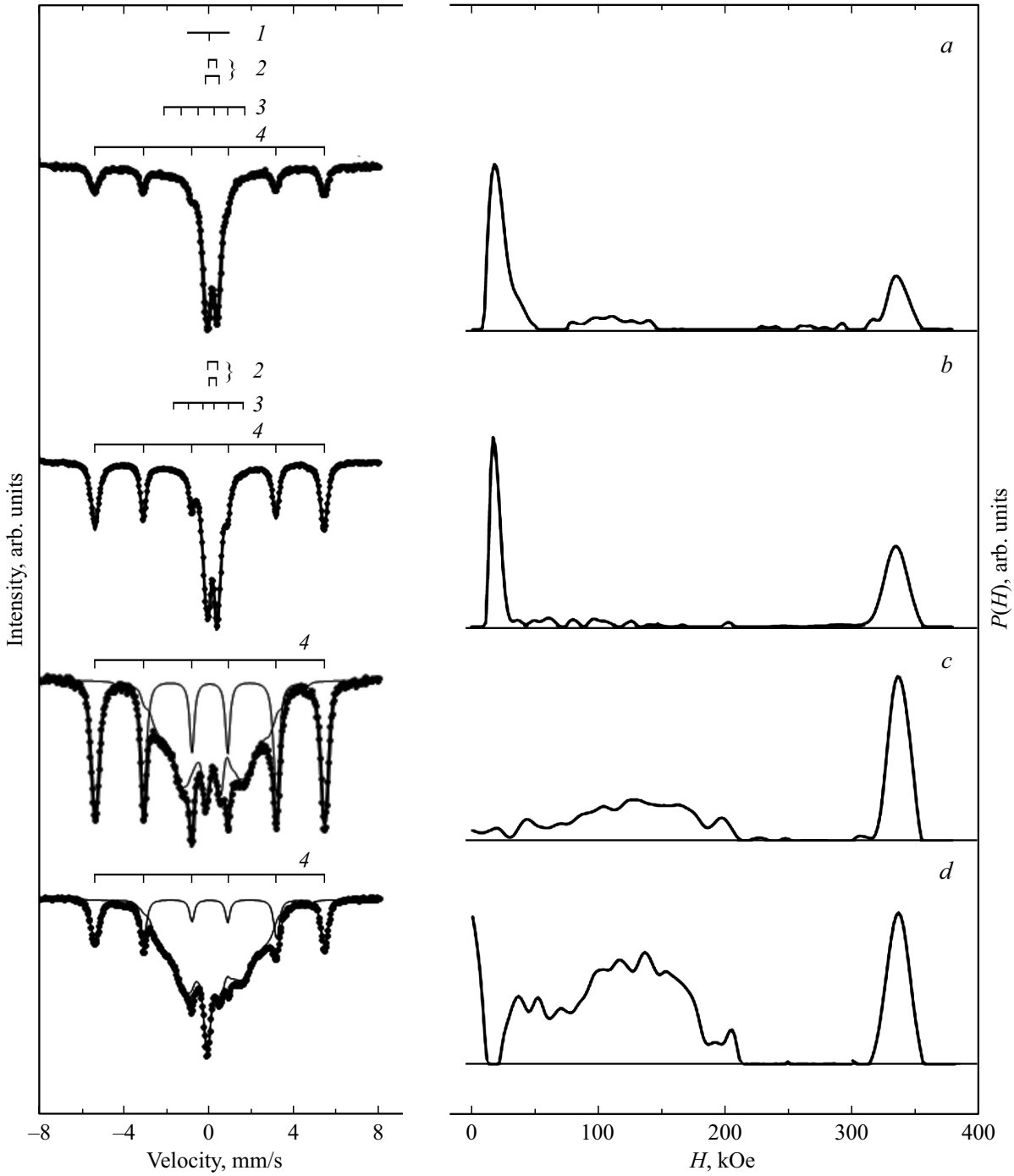

Figure 3. Mossbauer spectra (left) and distribution functions $P(H)$ (right) of alloys mechanosynthesized and annealed at 500°C: *a* — $(Fe_{0.80}Cr_{0.10}Ni_{0.10})_{83}C_{17}$; *b* — $(Fe_{0.85}Cr_{0.10}Ni_{0.05})_{83}C_{17}$; *c* — $(Fe_{0.90}Cr_{0.05}Ni_{0.05})_{83}C_{17}$; *d* — $(Fe_{0.85}Cr_{0.05}Ni_{0.10})_{83}C_{17}$. Components: *1* — paramagnetic austenite, *2* — paramagnetic cementite, *3* — ferromagnetic austenite, *4* — ferrite.

of the composite is in a multi-domain state. It is known that exchange interactions occur between ferromagnetic phases in direct contact. In particular, exchange interactions with neighboring ferromagnetic phases lead to a non-uniform distribution (bending, vortex, wagging, etc.) of magnetization in single-domain ferromagnetic particles. The magnetization reversal of such particles during measuring the coercive force is carried out by incoherent rotation of magnetization also in lower, as compared with coherent rotation, magnetic fields [19]. Therefore, single-domain ferrite inclusions of low-chromium composites annealed at 500°C (Figure 5, curve *2*) during the measurement process H_c are subjected to magnetization reversal by incoherent rotation in the field of coercive force of ferromagnetic cementite. As a result, H_c of low-chromium composites will be mainly determined by the coercivity

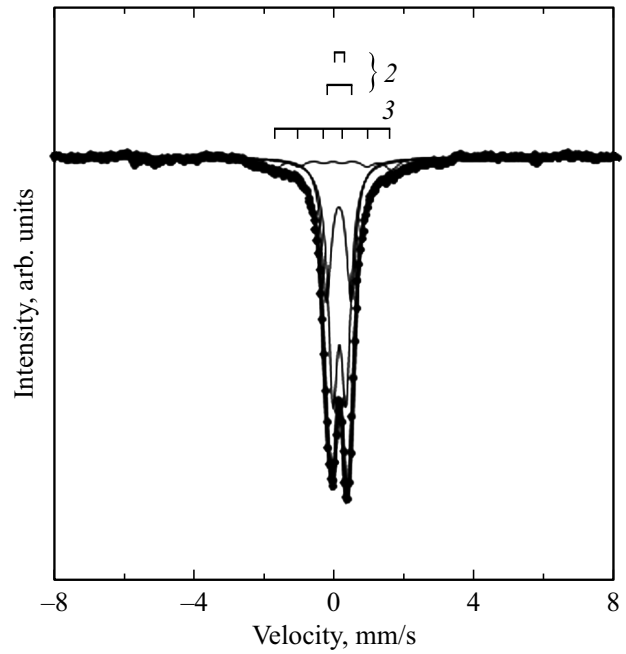

Figure 4. Mössbauer spectrum of mechanosynthesized and annealed at 500°C alloy $(Fe_{0.85}Cr_{0.10}Ni_{0.05})_{83}C_{17}$ considering subtraction of spectrum component from ferrite. Components: *2* — paramagnetic cementite, *3* — ferromagnetic austenite. Designations as in Figure 3, *b*.

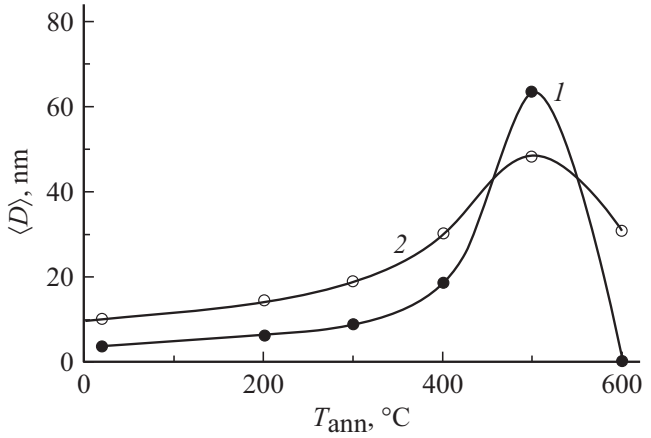

Figure 5. Average size of coherent scattering regions $\langle D \rangle$ of ferrite vs. annealing temperature T_{ann} of alloys: *1* — $(Fe_{0.80}Cr_{0.10}Ni_{0.10})_{83}C_{17}$, *2* — $(Fe_{0.05}Cr_{0.05}Ni_{0.10})_{83}C_{17}$.

of cementite. In this case the value H_c of cementite is determined by two factors. Firstly, by structural state of cementite [6]. Secondly, by the interaction (pinning) of cementite domain walls with various types of defects in the crystal structure.

Let's evaluate possible value of coercive force of cementite in discussed low-chromium composites according paper [7], which measured H_c of mechanosynthesized alloys with composition of cementite $(Fe_{0.95}Cr_{0.05})_{75}C_{25}$ and $(Fe_{0.93}Cr_{0.07})_{75}C_{25}$. After annealing at 500°C the cementite content in the alloys was close to 100%, and their H_c was 186 and 147 A/cm, respectively. The cementite of the studied composites is doped by chromium, according to our estimates, slightly higher than in [7]. Besides, cementite also contains Ni atoms, this also reduces the coercive force of cementite doped by chromium and nickel [20]. So, the coercive force of low-chromium composites after annealing at 500°C is $H_c = 100$ A/cm (Figure 2, *b*, curves *1, 2*), this is in satisfactory agreement with estimates H_c of cementite doped by Cr and Ni according to papers [7,20]. In this case, the dependence $H_c(T_{ann})$ of low-chromium composites in the range of T_{ann} 400 to 500°C is determined by a change in the structural state of cementite [6]. With T_{ann} increasing from 500 to 700°C value H_c of such composites decreases (Figure 2, *b*, curves *1, 2*), which first of all is due to decrease in defects density of crystalline structure of cementite [5].

Coercive force of all alloys, excluding $(Fe_{0.90}Cr_{0.05}Ni_{0.05})_{83}C_{17}$, in range T_{ann} from 600–700 to 800°C again increases (Fig 2, *b*, curves *2–4*). It is known that at elevated heating temperatures and holding at these temperatures, some part of the cementite can dissolve in austenite. During cooling cementite is separated from the austenite of the alloys under discussion (for the purposes of this article, we will call it „secondary") with reduced Cr content compared to the initial („primary") cementite formed during MS and subsequent annealing.

This can be proved, for example, by the dependence of the relative magnetic susceptibility on temperature measurements of $\chi/\chi_{20}(T)$, taken during cooling of composite samples $(Fe_{0.80}Cr_{0.10}Ni_{0.10})_{83}C_{17}$ after annealing at $T_{ann} = (600–800)$°C (Figure 6). Temperatures of curve maxima *1–3* correspond to Curie points $T_C \approx 60$, 120 and 170°C of ferromagnetic „secondary" cementite annealed at $T_{ann} = 600$, 700 and 800°C, respectively. From the data obtained it follows that with annealing temperature increasing, the Curie temperature of secondary cementite

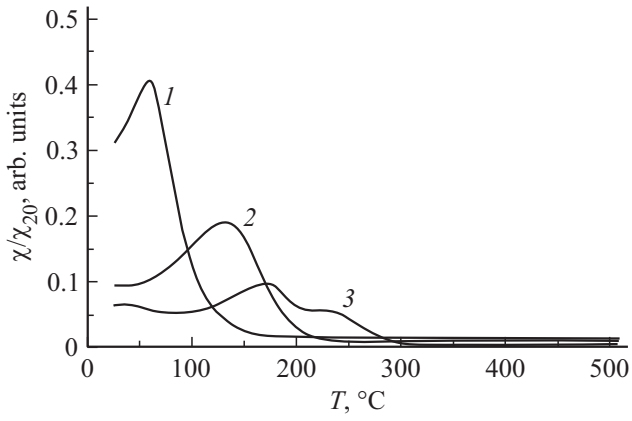

Figure 6. Relative magnetic susceptibility vs. measurement temperature $\chi/\chi_{20}(T)$, measured during cooling of alloy $(Fe_{0.80}Cr_{0.10}Ni_{0.10})_{83}C_{17}$ after annealing at temperature T_{ann}: *1* — 600; *2* — 700; *3* — 800°C. Here χ — current value of susceptibility; χ_{20} — value of susceptibility at 20°C, obtained during heating from initial temperature.

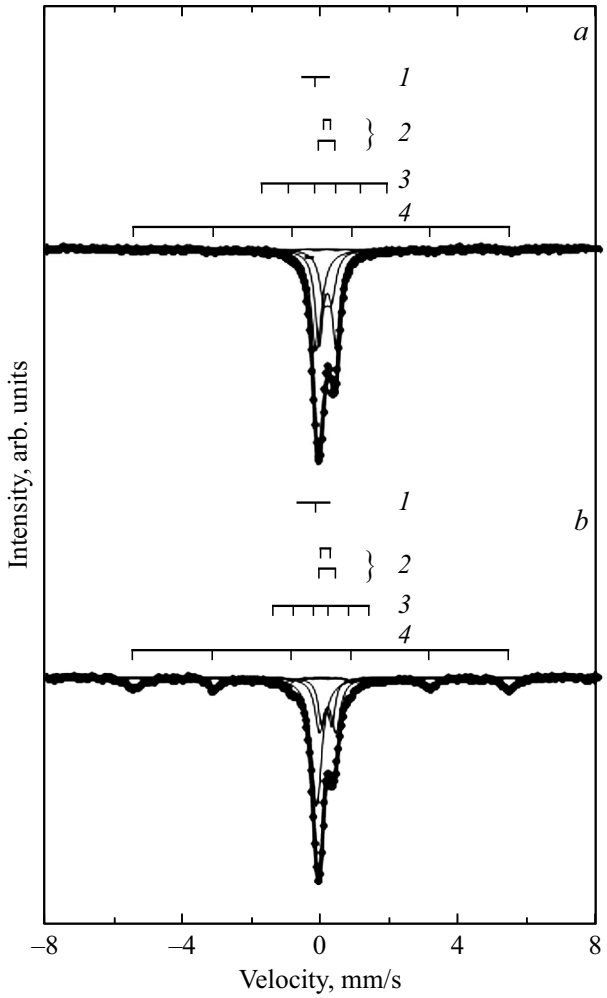

Figure 7. Mössbauer spectra of alloys mechanosynthesized and annealed at 800°C: *a* — $(Fe_{0.80}Cr_{0.10}Ni_{0.10})_{83}C_{17}$; *b* — $(Fe_{0.85}Cr_{0.05}Ni_{0.10})_{83}C_{17}$. Components: *1* — paramagnetic austenite, *2* — paramagnetic cementite, *3* — ferromagnetic cementite, *4* — ferrite.

increases. Taking into account [7], we can conclude that „secondary" cementite of the composite with increase in T_{ann} contains less chromium and, therefore, has higher values H_c.

The coercive force of composites depends not only on the coercivity of cementite, but also on the magnetic state of the phases surrounding it. Figure 7, *a* and *b* shows Mössbauer spectra of annealed at 800°C high-chromium $(Fe_{0.80}Cr_{0.10}Ni_{0.10})_{83}C_{17}$ and low-chromium $(Fe_{0.85}Cr_{0.05}Ni_{0.10})_{83}C_{17}$ alloys, respectively. The results of the analysis of Mössbauer spectra in discrete representation are given in Table 1 *b*. From Tables it follows that the fraction of iron atoms in paramagnetic phases (austenite and residues of „primary" cementite after separation from it of „secondary" cementite) of alloys $(Fe_{0.80}Cr_{0.10}Ni_{0.10})_{83}C_{17}$ and $(Fe_{0.85}Cr_{0.05}Ni_{0.10})_{83}C_{17}$ is 95 and 79%, respectively. All phases of these alloys have similar magnetic state. The difference is observed only in the Fe content in the phases: low-chromium alloy contains more Fe atoms in paramagnetic austenite and ferrite, and less in paramagnetic cementite. Ferrite in alloy $(Fe_{0.85}Cr_{0.05}Ni_{0.10})_{83}C_{17}$ again appears after annealing at elevated temperatures 700−800°C due to cementite disintegration. The content of Fe atoms in „secondary" cementite of both alloys is approximately the same and amounts to 3−4%. Similar results were obtained for the annealed alloy $(Fe_{0.85}Cr_{0.10}Ni_{0.05})_{83}C_{17}$. The only difference is that as a result of annealing at 800°C part of the austenite transforms into martensite (Figure 1, *b*). Thus, the coercive force of the low-chromium alloy $(Fe_{0.85}Cr_{0.05}Ni_{0.10})_{83}C_{17}$ and alloys with high-chromium content annealed at temperatures 700−800°C, will be mainly determined by the coercivity of ferromagnetic inclusions of secondary cementite surrounded by paramagnetic phases, H_c of which increases with annealing temperature increasing, as well as ferrite or martensite separation increasing.

The coercive force H_c of low-doped composite $(Fe_{0.90}Cr_{0.05}Ni_{0.05})_{83}C_{17}$ with annealing temperature rise from 500°C and up to 800°C decreases monotonically (curve *1*, Figure 2, *b*). Let's discuss possible reasons of H_c decreasing of alloy samples annealed in range $T_{ann} = 700-800$°C. To determine the reasons of such behavior of H_c information is required on magnetic state of this alloy phases. Figure 8 shows the Mössbauer spectrum of the alloy under discussion, obtained after annealing at $T_{ann} = 800$°C, and the function $P(H)$, reflecting the distribution from the atoms of the immediate environment of hyperfine magnetic fields on the nuclei of Fe isotopes located in phases. Since the sample composition consists mainly of ferromagnetic phases, it is more convenient to discuss them on the basis of analysis of the function $P(H)$ of the alloy. From the analysis of the function $P(H)$ it follows that 5% of all Fe atoms contained in the alloy are in paramagnetic austenite (the maximum of the function $P(H)$ is located in the field of $H = 0$ kOe). In martensite (maximum of the function $P(H)$ is in the field of 337 kOe) 40% of iron atoms were found. Ferromagnetic cementite (distribution of function $P(H)$ in the field range $H = 50-180$ kOe) contains 49% of Fe atoms. The remaining $\approx 6\%$ of Fe atoms are

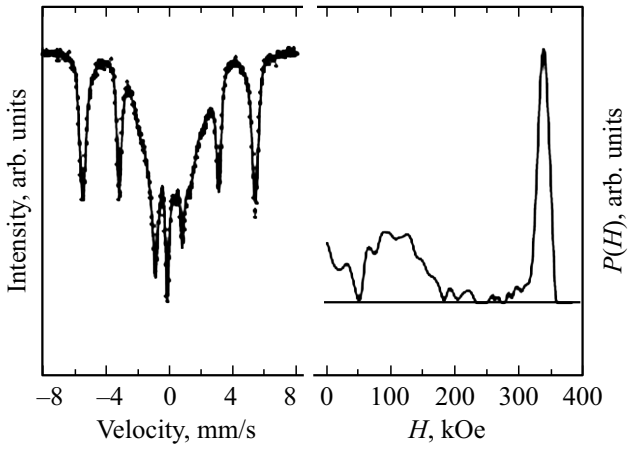

Figure 8. Mössbauer Spectrum (left) and function $P(H)$ (right) of composite $(Fe_{0.90}Cr_{0.05}Ni_{0.05})_{83}C_{17}$ after annealing at 800°C.

most likely located in paramagnetic or weakly ferromagnetic cementite.

All available cementite in lightly doped alloy, annealed at temperatures of 700−800°C, can be divided into two parts. The first, main part of its total volume is the residues of „primary" cementite after „secondary" cementite separation from it. And the second part, actually „secondary" cementite in a small amount. The coercive force and saturation magnetization σ_s of „secondary" cementite increase with T_{ann} increasing. At the same time, H_c and σ_s of residues of „primary" cementite, on the contrary, decrease due to, although insignificant but increase in the concentration of doping elements in it. During annealing, there is an intensive decrease in the density of defects in the crystalline structure of all cementite, which leads to decrease in its coercive force. A combined influence of these factors mainly results in coercive force decreasing of nanocomposite $(Fe_{0.90}Cr_{0.05}Ni_{0.05})_{83}C_{17}$ after annealing in temperature range of 700−800°C. The martensite appearance most likely slightly increases the coercive force of the composite under discussion, annealed at $T_{ann} = 800$°C, but does not change the nature of the dependence $H_c(T_{ann})$ in the annealing temperature range 700−800°C.

Thus, magnetic and Mössbauer measurements, in addition to X-ray diffraction, provide more comprehensive information about the phase composition, magnetic state and doping of the phases of the studied composites based on the Fe-C system. The information obtained allows us to understand the reason for the difference in the magnetic hysteretic properties of nickel-doped high- and low-chromium composites, which is formed as a result of heat treatment of these alloys.

4. Conclusions

1. Magnetic properties of high-chromium $(Fe_{0.90-y}Cr_{0.10}Ni_y)_{83}C_{17}$ and low-chromium $(Fe_{0.95-y}Cr_{0.05}Ni_y)_{83}C_{17}$ nanocomposites are studied, where $y = 0.05$, 0.10, after mechanosynthesis and subsequent annealing depending on phase composition and structural state of phases.

2. The dependences of the coercive force H_c of the studied alloys on the annealing temperature are curves with maximum at $T_{ann} \approx 500$°C. The maximum coercive force H_c of high-chromium composites reaches values of (210−240) A/cm, which by more than two times exceeds the maximum values H_c of low-chromium composites. This ratio H_c of composites is determined by the magnetic and structural state of their phases. It was shown that after annealing at 500°C the high-chromium composites are a matrix, mainly of paramagnetic cementite, in which there exist nanoscale ferrite inclusions. In low-chromium nanocomposites annealed at 500°C the nanoscale ferrite inclusions are surrounded by ferromagnetic cementite.

3. To explain the maximum values H_c of high-chromium composites, it was suggested that after annealing at 500°C the inclusions of the ferrite phase have average size close to the critical single-domain size. During measuring the coercive force H_c the magnetization reversal of single-domain ferrite inclusions located in matrix of paramagnetic phases occurs through irreversible coherent rotation of magnetization. This provides high value of the coercive force of single-domain ferrite inclusions and, consequently, high values of H_c of high-chromium composites. In low-chromium nanocomposites the single-domain ferrite inclusions are located in the environment of multi-domain ferromagnetic cementite. The coercive force of such alloys is determined by another mechanism. Magnetization reversal is performed by incoherent rotation in the field of the coercive force of ferromagnetic cementite, which ensures maximum value of their $H_c \approx 100$ A/cm.

4. The decrease in coercive force H_c of the studied nanocomposites in the annealing temperature range of 500 to 600−700°C occurs mainly due to decrease in the content and size of ferrite phase inclusions, as well as decrease in the defects density in the crystalline structure of cementite.

5. Some increase of H_c of all, excluding $(Fe_{0.90}Cr_{0.05}Ni_{0.05})_{83}C_{17}$, composites, in range T_{ann} of 700 to 800°C was due to mainly occurrence during cooling after annealing of the ferromagnetic „secondary" cementite surrounded by paramagnetic phases. The chromium content in such cementite decreases with annealing temperature increase T_{ann}, and its coercive force increases.

Funding

The study was carried out using the equipment of the Shared Use Center „Center of Physical and Physicochemical Methods of Analysis and Study of Properties and Characteristics of the Surface, Nanostructures, Materials and Products" of the Udmurt Federal Research Center of the Ural Branch of RAS within the framework of the state task of the Ministry of Science and Higher Education of the Russian Federation (No. of state registration 121030100003-7).

Conflict of interest

The authors declare that they have no conflict of interest.

References

[1] L.I. Svistun. Izv. vuzov. Poroshkovaya metallurgiya i funktsional'nye pokrytiya, *3*, 41 (2009). (in Russian).
[2] T.G. Langdon. Acta Mater. **61**, *19*, 7035 (2013).
[3] C. Suryanarayana, N. Al-Aqeeli. Prog. Mater. Sci. **58**, *4*, 383 (2013).
[4] E.P. Elsukov, V.M. Fomin, D.A. Vytovtov, G.A. Dorofeev, A.V. Zagainov, N.B. Arsentieva, S.F. Lomaeva. FMM **100**, *3*, 56 (2005). (in Russian).
[5] E.P. Elsukov, A.I. Ul'yanov, A.V. Zagainov, N.B. Arsent'eva. JMMM **258**−**259**, 513 (2003).
[6] A.K. Arzhnikov, L.V. Dobysheva, C. Demmangeat. J. Phys.: Condens. Mater. **19**, 19 (2007).
[7] A.A. Chulkina, A.I. Ulyanov, A.L. Ulyanov, I.A. Baranova, A.V. Zagainov, E.P. Elsukov. FMM **116**, *1*, 21 (2015). (in Russian).

[8] F. Zhao, O. Tegus, B. Fuquan, E. Brück. Int. J. Minerals Metallurgy Mater. **16**, *3*, 314 (2009).
[9] A.I. Ulyanov, A.A. Chulkina, V.A. Volkov, A.L. Ulyanov, A.V. Zagajnov. FMM **118**, *7*, 725 (2017). (in Russian)
[10] T. Shigematsu. J. Phys. Soc. Jpn. **37**, *4*, 940 (1974).
[11] A.I. Ulyanov, A.A. Chulkina, V.A. Volkov, A.L. Ulyanov, A.V. Zagajnov. Materialovedenie *12*, 17 (2020). (in Russian)
[12] E.V. Voronina, N.V. Ershov, A.L. Ageev, Yu.A. Babanov. Phys. Status Solidi B **160**, *2*, 625 (1990).
[13] A.A. Chulkina, A.I. Ulyanov, V.A. Volkov, A.L. Ulyanov, A.V. Zagajnov. ZhTF **65**, *5*, 787 (2020). (in Russian).
[14] V.A. Shabashov, V.V. Sagaradze, A.V. Litvinov, A.E. Zamatovsky. FMM **116**, *9*, 918 (2015). (in Russian)
[15] J.M.D. Coey. Magnetism and Magnetic Materials. Cambridge University Press, Cambridge (2010). 633 p.
[16] V.I. Petinov. Tech. Phys. **59**, *1*, 6 (2014)
[17] R.Z. Valiev, I.V. Alexandrov. Nanostrukturnye metally, poluchennye intensivnoj plasticheskoj deformatsiej. Logos, M. (2000). 272 s. (in Russian).
[18] E.P. Elsukov, G.A. Dorofeev, V.V. Boldyrev. Dokl. AN **391**, *5*, 640 (2003). (in Russian).
[19] S.I. Vonsovskij. Magnetizm. Nauka, M., (1971). 805 s. (in Russian).
[20] A.A. Chulkina, A.I. Ulyanov, A.L. Ulyanov. Khimicheskaya fizika i mezoskopiya **22**, *2*, 230 (2020). (in Russian).

Translated by I.Mazurov